Journal of Materials Chemistry A

PAPER

View Article Online
View Journal | View Issue

Published on 07 February 2017. Downloaded by Osaka University on 20/12/2017 11:40:28.

Cite this: J. Mater. Chem. A, 2017, 5, 5106

A 1,1′-vinylene-fused indacenodithiophene-based low bandgap polymer for efficient polymer solar cells†

Qunping Fan,‡[a] Wenyan Su,‡[a] Xia Guo,*[a] Xi Zhang,[b] Zhuo Xu,[a] Bing Guo,[a] Lang Jiang,[b] Maojie Zhang*[a] and Yongfang Li*[ab]

Received 31st December 2016
Accepted 6th February 2017

DOI: 10.1039/c6ta11240d

rsc.li/materials-a

A 1,1′-vinylene-fused indacenodithiophene (**IDTV**) donor unit with 22 π-conjugated electrons was synthesized. A ladder-type D–A copolymer **PIDTV-ffBT** using **IDTV** as the donor unit and 5,6-difluorobenzothiadiazole (ffBT) as the acceptor unit was developed for application as a donor material in polymer solar cells (PSCs). Compared to other analogue polymers, **PIDTV-ffBT** possesses a two-dimensional conjugated multi-electron fused ring, excellent planarity and close π–π stacking, leading to a higher light harvesting coefficient, an enhanced charge carrier mobility of 0.032 $cm^2\ V^{-1}\ s^{-1}$ and improved photovoltaic performance. The PSCs based on **PIDTV-ffBT**:$PC_{71}BM$ achieved a promising power conversion efficiency (PCE) of 7.3% with a high short-circuit current density (J_{sc}) of 17.1 mA cm^{-2}. These results indicate that the introduction of the 1,1′-vinylene-fused system into **IDTV** for ladder-type polymers is an effective strategy to enhance the light absorption coefficient and improve charge carrier mobility for high efficiency PSCs.

Introduction

As a promising renewable energy source technology, solution-processed polymer solar cells (PSCs) based on p-type conjugated polymers as electron donors and n-type fullerene derivatives as electron acceptors with a nanoscale phase-separated bulk heterojunction (BHJ) morphology have attracted considerable attention due to their advantages of flexibility and potentially inexpensive large area manufacturing.[1–4] Over the past few years, rapid progress has been made in this field. Power conversion efficiencies (PCEs) of more than 10% for traditional single-junction PSCs[5–8] and over 11% for tandem PSCs[9–11] have been achieved. As is well known, the key factors that determine the PCE of PSCs are the open-circuit voltage (V_{oc}), short-circuit current density (J_{sc}), and fill factor (FF).[12–15] These parameters are closely related to the optical and electrical properties of the polymer donors and the blend morphology of the active layer in BHJ PSCs. Among conjugated polymer donors, donor–acceptor (D–A) alternating conjugated polymers attract great interest because of their tunable properties including their optical absorption band, molecular energy level and hole mobility.[16–20] PSCs based on D–A copolymers have made great progress with PCEs over 10%.[5–7]

Indacenodithiophene (IDT) as a promising electron-rich donor unit has attracted considerable attention and has been widely used in BHJ PSCs due to its high degree of rigidity and planarity and unique heteroaromatic ladder-type structure.[21–28] So far, PSCs based on IDT-containing polymer donors have exhibited PCEs over 7%.[21,22] However, the relatively narrow absorption spectra of these polymers are their weak point which limit the J_{sc} and PCE of the corresponding PSCs. In order to enhance the light-harvesting capacity of IDT-based polymers, great efforts have been made, such as changing the bridging atoms of the backbone or modifying the side chains of the IDT unit.[23,24] However, these methods are not effective in broadening the absorption spectra of these polymers. Another common way to strengthen the optical absorption of IDT-based polymers is to extend the conjugation length of the IDT backbone.[22,25] For example, Jen *et al.* reported an IDT derivative with an extended π-conjugated skeleton, IDTT, that is fused to two thiophene rings on both sides of the IDT unit.[22a] Compared with IDT-based polymers,[23,26] IDTT-based polymers exhibit a higher extinction coefficient, resulting from their enhanced planarity, but the absorption region of the polymers still changes little. From the structure of the IDT unit, it can be clearly found that the sp^3-hybridized carbon at 4,9-positions only plays the role of forming the fused rings, but does not contribute electrons to the

[a]State and Local Joint Engineering Laboratory for Novel Functional Polymeric Materials, Laboratory of Advanced Optoelectronic Materials, College of Chemistry, Chemical Engineering and Materials Science, Soochow University, Suzhou 215123, China. E-mail: mjzhang@suda.edu.cn; guoxia@suda.edu.cn; liyongfang@suda.edu.cn

[b]Beijing National Laboratory for Molecular Sciences, CAS Key Laboratory of Organic Solids, Institute of Chemistry, Chinese Academy of Sciences, Beijing 100190, China. E-mail: liyf@iccas.ac.cn

† Electronic supplementary information (ESI) available. See DOI: 10.1039/c6ta11240d

‡ These authors contributed equally to this work.

This journal is © The Royal Society of Chemistry 2017

Published on 07 February 2017. Downloaded by Osaka University on 20/12/2017 11:40:28.

π-conjugated system of the backbone.[29] Hence, to enhance the π electron delocalization of side chains on the IDT unit is a potential strategy to improve the light harvesting capacity of the polymers and hence achieve a higher J_{sc} and PCE for PSCs.

In this work, we synthesized a five-membered fused-ring donor unit with 22 π-electrons, **IDTV**, where the 4,9-positions of the IDT unit are fused with two vinylene groups (Scheme 1a). Compared to the IDT unit, the **IDTV** unit possesses a more extended conjugation in the vertical direction and more π-conjugated electrons, which will facilitate π-electron delocalization along the polymer backbone and thus reduce its optical bandgap. In addition, alkyl chains far from the skeleton of the **IDTV** unit can promote the rigid and coplanar structural properties of the resulting polymers to prevent rotational disorder and reduce the reorganization energy, which will be beneficial to enhance carrier mobility.[22,25] Furthermore, the D–A copolymer **PIDTV-ffBT** (see Scheme 1b) based on **IDTV** as the donor unit and 5,6-difluorobenzothiadiazole (ffBT) as the acceptor unit was synthesized for application as a donor material in PSCs. Generally, the broadening of the absorption spectra of polymers tends to up-shift the HOMO level, which will reduce the open circuit voltage (V_{oc}) of the related devices.[13,18a] Therefore, compared to the similar polymer CIDT,[23a] we introduced two fluorine atoms in the benzothiadiazole (BT) unit to down-shift the HOMO level of the polymer. As we expected, compared to the analogue polymers,[22–26] **PIDTV-ffBT** shows a broader absorption in the wavelength range of 300–810 nm with a lower optical bandgap (E_g^{opt}) of 1.53 eV, a high extinction coefficient of 1.34×10^5 cm^{-1} at 717 nm, and a hole mobility of 0.032 cm^2 V^{-1} s^{-1}. As a result, the PSCs based on **PIDTV-ffBT**:$PC_{71}BM$ exhibit an optimized PCE of 7.3% with a V_{oc} of 0.70 V, a J_{sc} of 17.1 mA cm^{-2}, and a FF of 61%. These PCE and J_{sc} values are the highest values reported in the literature so far for PSCs based on IDT-*alt*-BT copolymers.[22–26] Moreover, the J_{sc} of 17.1 mA cm^{-2} is comparable to those of PSCs based on DPP-based[13,30] and TT-based[4b,7,20] low bandgap polymers, and is the highest J_{sc} value reported to date for PSCs based on IDT-containing polymers as donors.[21–28]

Results and discussion

Synthesis and thermal properties of PIDTV-ffBT

As shown in Scheme 1b, **IDTV** was prepared through an addition reaction with the participation of a Grignard reagent and an elimination reaction under acidic conditions according to the procedure in the literature.[31] Compound **IDTV-Sn** was obtained by the reaction of tin reagents at low temperature. The polymer **PIDTV-ffBT** was synthesized by palladium catalyzed Stille-coupling polymerization with a yield of 73%. The number average molecular weight (M_n) and polydispersity index (PDI) of **PIDTV-ffBT** were 28.0 kDa and 3.24, respectively, as estimated by gel permeation chromatography (GPC) using 1,2,4-trichlorobenzene as the eluent

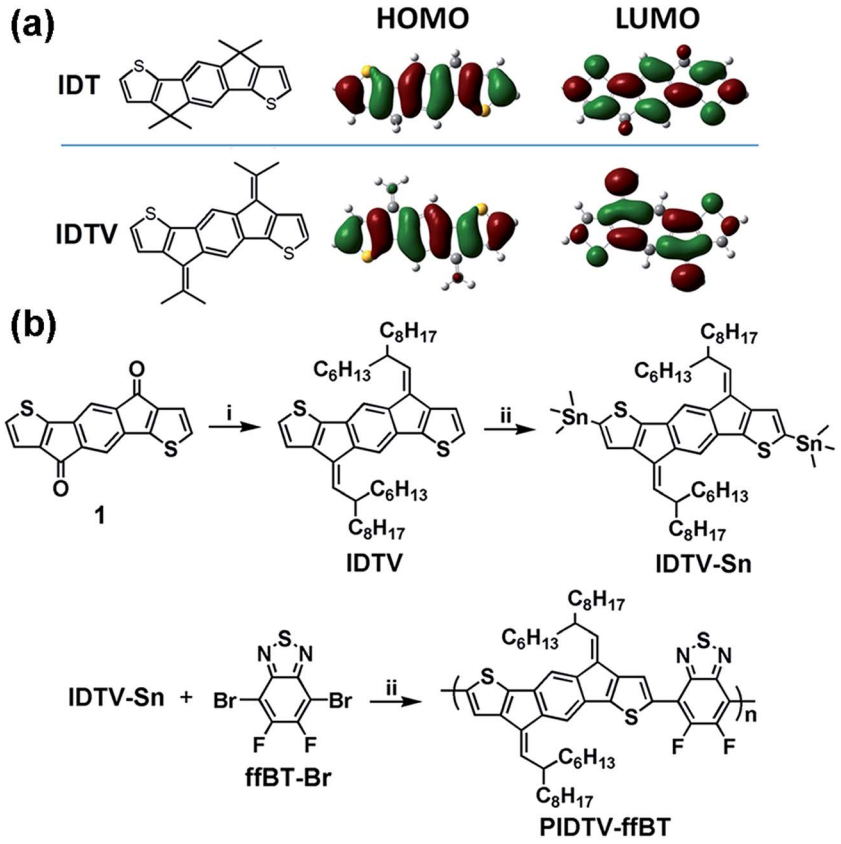

Scheme 1 (a) HOMO and LUMO distribution modes of IDT and **IDTV** obtained using DFT calculations; (b) synthetic route and molecular structure of **PIDTV-ffBT**.

Published on 07 February 2017. Downloaded by Osaka University on 20/12/2017 11:40:28.

at a high temperature of 160 °C. The large PDI value may be due to the planar structure of the **IDTV** unit which reduces the solubility of the polymer. The polymer shows good solubility in high temperature halogen organic solvents such as chlorobenzene and *o*-dichlorobenzene (*o*-DCB). In the thermogravimetric analysis (TGA), the polymer displays a thermal decomposition temperature of 376 °C (see Fig. S1 in the ESI†) at 5% weight loss, which indicates a good thermal stability for PSC application.

Absorption spectra and electronic energy levels

The UV-vis absorption spectra of **PIDTV-ffBT** in *o*-DCB solution (1×10^{-5} M) and solid films are shown in Fig. 1a. In solution, the absorption spectrum of the polymer exhibits strong absorption in the 500–750 nm region with a maximum absorption peak (λ_{max}) at 695 nm. In the solid film, the maximum absorption peak is red-shifted to 716 nm with an absorption coefficient of 1.34×10^5 cm^{-1} (Fig. 1a), due to the strong intermolecular π–π stacking interaction of the polymer. **PIDTV-ffBT** shows an optical bandgap (E_g^{opt}) of 1.53 eV estimated from the absorption edge (810 nm) of its thin film, which is comparable to that of DPP-based polymers.[13,30] Furthermore, compared to the IDT-*alt*-BT-based analogue polymers ($\lambda_{max} \approx$ 620–650 nm and $E_g^{opt} \approx$ 1.76–1.78 eV),[22–26] **PIDTV-ffBT** shows a red shift of the absorption peak and the absorption edge and a higher extinction coefficient. This phenomenon indicates that a strong intramolecular charge transfer (ICT) effect exists between the **IDTV** and ffBT units, due to the increase of the electron-donating ability by fusing two vinylene groups at the 1,1′-positions of the **IDTV** unit (Scheme 1a). Thus a high J_{sc} is expected in the PSCs with the polymer as the donor material.

Electrochemical cyclic voltammetry (CV) was carried out to estimate the energy levels of the polymer (Fig. 1b). The highest occupied molecular orbital (HOMO) and the lowest unoccupied molecular orbital (LUMO) levels estimated from the onset of oxidation and reduction potentials (E_{ox}/E_{red}, 0.52/−1.02 V *vs.* Ag/Ag$^+$) for **PIDTV-ffBT** are −5.23/−3.69 eV according to the empirical equations:[13b] HOMO $= -e(E_{ox} + 4.71)$ (eV), and LUMO $= -e(E_{red} + 4.71)$ (eV), respectively. Moreover, the electrochemical bandgap (E_g^{cv}) of **PIDTV-ffBT** is 1.54 eV, which is almost identical to its E_g^{opt}.

Theoretical calculations

Theoretical calculations of the polymer were carried out by the density functional theory (DFT) method with a B3LYP/6-31G*(d,p) basis set. As shown in Fig. 2a, the HOMO is delocalized along the whole π-conjugated backbone while the LUMO is mostly concentrated on the acceptor groups. These results indicate the formation of a well-defined D–π–A structure and the intramolecular charge transfer behavior of the material. As shown in Fig. 2b, the polymer backbone displays an almost straight line side view, which means that it has an outstanding planar structure. Moreover, the polymer backbone also shows a dominant continuous positive electrostatic potential (ESP), as shown in Fig. 2c.

XRD analysis and charge carrier mobilities

Meanwhile, the X-ray diffraction (XRD) pattern was measured to study the crystallinity and molecular packing of the pure polymer film, as shown in Fig. 2d. A sharp and strong (100) diffraction peak at $2\theta = 5.10°$, corresponding to a *d*-spacing of 17.4 Å, is observed in the XRD pattern of the pure polymer film. This is a smaller lamellar spacing compared with those of the most widely used polymers such as PTB7 (>18 Å)[32a] and PCDTBT (>21 Å).[32b] Notably, there is a clear diffraction peak at $2\theta = 25.3°$, corresponding to the (010) π–π stacking with a *d*-spacing of 3.51 Å, which is obviously lower than that of IDT-*alt*-BT-based conjugated polymer analogues (3.8–4.1 Å).[23a,33] The nearly flat polymer skeleton, continuous positive ESP, and small lamellar spacing and π–π stacking spacing are conducive for **PIDTV-ffBT** to achieve high carrier mobility.[34]

To estimate the hole mobility of **PIDTV-ffBT**, bottom-gate/bottom-contact organic field-effect transistors (OFET) were fabricated. Fig. S2 in the ESI† shows the corresponding output and transfer curves of the **PIDTV-ffBT**-based OFET devices. The on–off ratio is 3.9×10^4 with a threshold voltage (V_t) of 12.5 V. The OFET hole mobility of **PIDTV-ffBT** is as high as 0.032 cm^2 V^{-1} s^{-1}. The results confirm our design concept, that is, the extension of the effective conjugation length and the improvement of the planarity can promote intermolecular chain packing and charge transport. Notably, the hole mobility of

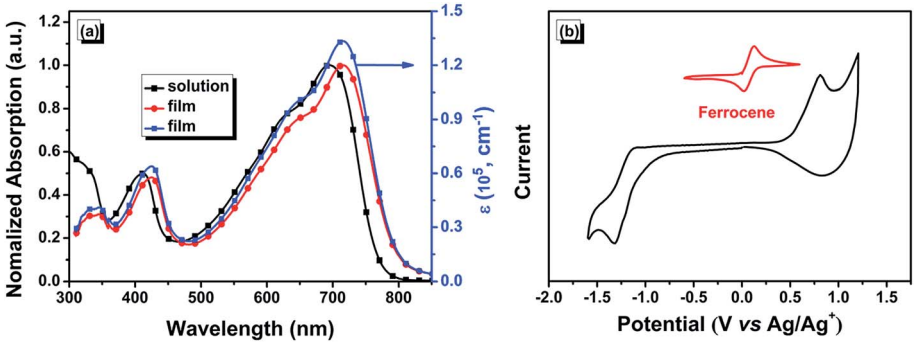

Fig. 1 (a) UV-vis absorption spectra of PIDTV-ffBT in *o*-DCB solution and films (the red line indicates the normalized absorption and the blue line indicates the extinction coefficient of the film); (b) cyclic voltammogram of the PIDTV-ffBT film on a glassy carbon electrode measured in a 0.1 mol L^{-1} Bu_4NPF_6 acetonitrile solution at a scan rate of 50 mV s^{-1}.

 This journal is © The Royal Society of Chemistry 2017

Published on 07 February 2017. Downloaded by Osaka University on 20/12/2017 11:40:28.

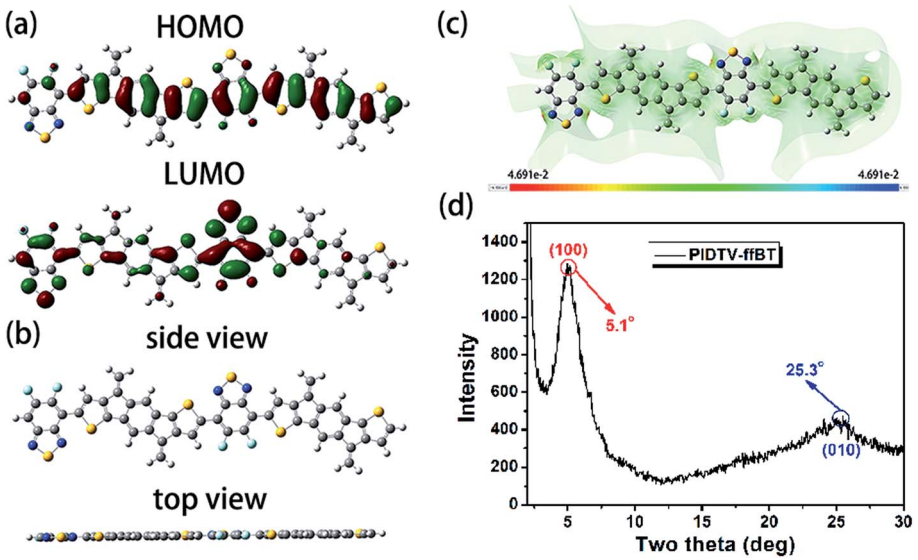

Fig. 2 Optimized geometries of **PIDTV-ffBT** by DFT calculations at the B3LYP/6-31G*(d,p) level: (a) the HOMO and LUMO electron distribution; (b) side view and top view; (c) map of the ESP surfaces based on DFT calculations; red color indicates greater negative charge, while blue color indicates greater positive charge. (d) XRD pattern of the pure **PIDTV-ffBT** film.

PIDTV-ffBT measured by the SCLC method is also up to 5.04 × 10^{-3} cm^2 V^{-1} s^{-1} (see Fig. S3 and Table S1 in the ESI†).

Photovoltaic properties

To investigate the photovoltaic properties of **PIDTV-ffBT**, PSCs were fabricated with a conventional device structure of ITO/PEDOT:PSS/**PIDTV-ffBT**:$PC_{71}BM$/$PrC_{60}MAIodide$ Salt/Al (see Fig. S4 in the ESI†) and were characterized under the illumination of AM 1.5G (100 mW cm^{-2}), where the commercially available $PrC_{60}MAIodide$ Salt was used as the cathode interfacial layer because of its high performance in PSCs.[14a] The effect of the donor/acceptor (D/A, **PIDTV-ffBT**:$PC_{71}BM$) weight ratios

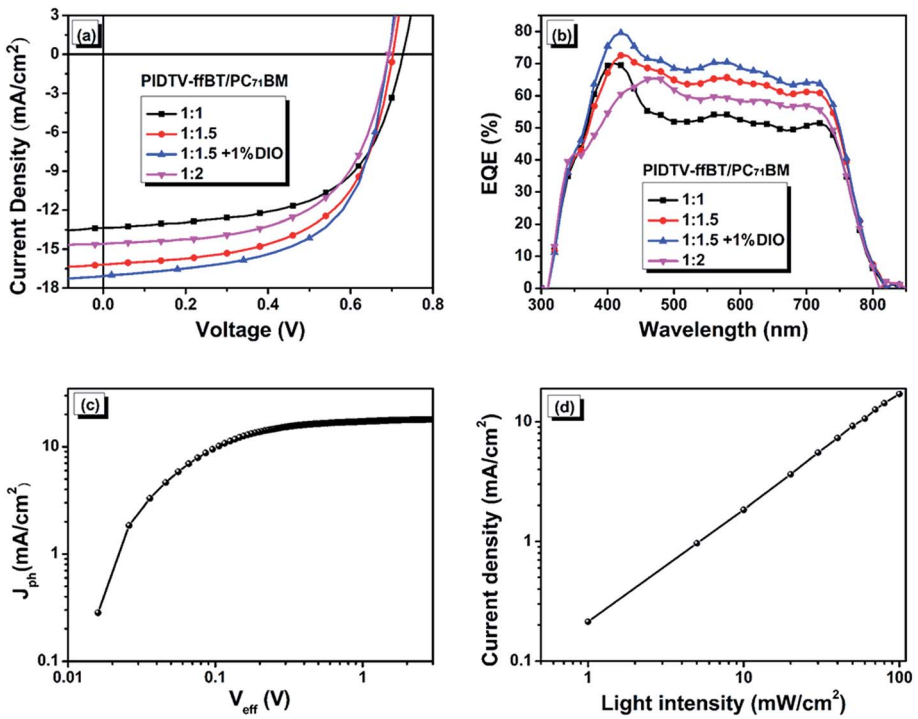

Fig. 3 (a) *J*–*V* curves of the PSCs based on **PIDTV-ffBT**:$PC_{71}BM$ with different D/A ratios (w/w) or with 1% DIO under AM 1.5G illumination (100 mW cm^{-2}); (b) EQE curves of the corresponding PSCs. (c) Photocurrent density (J_{ph}) *versus* effective voltage (V_{eff}) characteristics; (d) J_{ph} *versus* light intensity of the PSCs based on **PIDTV-ffBT**:$PC_{71}BM$ (1 : 1.5, w/w) with 1% DIO.

Published on 07 February 2017. Downloaded by Osaka University on 20/12/2017 11:40:28.

(w/w) in the active layer on device performance was first studied in the range of D/A weight ratios from 1 : 1 to 1 : 2 for the blends. Fig. 3a shows the current density–voltage (J–V) curves of the devices, and the corresponding device parameters are listed in Table 1. We found that the D/A ratio plays an important role in determining the device photovoltaic performance. All the PSCs with different D/A weight ratios in the active layer with a thickness of *ca.* 90 nm show good photovoltaic performance with an average PCE higher than 5.6%, an average J_{sc} higher than 13.2 mA cm^{-2}, and almost the same FF of *ca.* 59%. The optimum D/A weight ratio was found to be 1 : 1.5; the corresponding PSC showed the highest PCE of 6.7% with a V_{oc} of 0.70 V, a J_{sc} of 16.2 mA cm^{-2}, and a FF of 59%. Subsequently, the commonly used processing additive DIO with a high boiling point was used to optimize the morphology of the active layer for obtaining more efficient PSCs. Fig. S5 in the ESI† shows the J–V curves and EQE curves of the devices based on **PIDTV-ffBT**:$PC_{71}BM$ (1 : 1.5, w/w) with different DIO additive contents, and the corresponding device parameters are listed in Table S2 in the ESI.† We found that introducing DIO into the *o*-DCB blend solution can significantly improve the photovoltaic performance of the device. When 0.5% (v/v) DIO was added to the *o*-DCB blend solution, the PSC demonstrated a higher PCE of 7.1% benefitting from its higher J_{sc}, which increased from 16.2 to 17.4 mA cm^{-2}. The highest PCE of 7.3% with a V_{oc} of 0.70 V, a J_{sc} of 17.1 mA cm^{-2} and a FF of 61% was obtained for the PSCs with the treatment of 1% (v/v) DIO additive. To the best of our knowledge, the PCE of 7.3% and the J_{sc} of 17.4 mA cm^{-2} are among the highest values reported for PSCs with IDT-*alt*-BT-based polymers as donor materials.

Fig. 3b shows the external quantum efficiency (EQE) curves of the PSCs based on **PIDTV-ffBT**:$PC_{71}BM$ with different D/A weight ratios and with 1% DIO additive treatment. All devices show a broad EQE response in the wavelength range from *ca.* 300 to 810 nm. EQE values higher than 65% were observed in the range of 380–720 nm, and the maximum EQE value was close to 80% at 420 nm for the champion device with a D/A weight ratio of 1 : 1.5 and 1% DIO additive treatment, which indicates that the blend film (1 : 1.5, w/w) processed with 1% DIO has more efficient photon harvesting, exciton separating and charge transporting ability. According to the EQE curves and the solar irradiance spectrum, the mismatches between the integral J_{sc} values from the EQE curves and the measured J_{sc} values from J–V curves are below 3%.

To understand the main mechanisms involved in the **PIDTV-ffBT**:$PC_{71}BM$-based PSCs, the charge generation and extraction properties were studied. We measured the photocurrent density (J_{ph}) *versus* effective voltage (V_{eff}) of the PSCs, as shown in Fig. 3c. J_{ph} can be described as $J_{ph} = J_L - J_D$, where J_L and J_D are the photocurrent densities under illumination and in the dark, respectively. V_{eff} can be described as $V_{eff} = V_0 - V_{bias}$, where V_0 is the voltage at which the photocurrent is zero and V_{bias} is the applied external voltage bias.[34,35] Thus, V_{eff} determines the electric field in the bulk region and thereby determines the carrier transport and the photocurrent extraction. At high V_{eff} values, mobile charge carriers rapidly move toward the related electrodes with minimal recombination. J_{ph} reaches saturation (17.5 mA cm^{-2}) at $V_{eff} \geq 2$ V, which implies that all photogenerated charge carriers can be extracted by the electrodes. Under short-circuit conditions of the devices, J_{ph} is 17.1 mA cm^{-2}, which is comparable to that at high V_{eff}. Near the maximum power output point, recombination will be strongly competing with the carrier extraction as carriers slow down due to the reduced electric field. However, the J_{ph} of the PSCs based on **PIDTV-ffBT**:$PC_{71}BM$ (1% DIO) is still as high as 13.8 mA cm^{-2} at the maximum power point, $\approx$79% of all photogenerated carriers collected by the electrodes, indicating efficient photogenerated exciton dissociation and charge collection.

We also measured J_{sc} under different light intensities (P) to study the charge recombination under the short-circuit conditions of the cells (Fig. 3d). The relationship between J_{sc} and P can be defined as $J_{sc} \propto P^S$. If all free carriers are transported and collected at the electrodes prior to recombination, S should be equal to 1, while $S < 1$ indicates the existence of bimolecular recombination.[36] In logarithmic coordinates, the J_{sc} shows a linear dependence on the light intensity with a slope (S) of 0.96, indicative of efficient charge transportation and negligible bimolecular recombination.

In order to understand the effect of DIO additive on the photovoltaic performance of the device, the charge mobilities were measured by the SCLC method.[14] As shown in Fig. S3 and Table S1 in the ESI,† the blend films processed with 1% DIO exhibited higher hole mobility and electron mobility (4.13×10^{-4} and 1.57×10^{-3} cm^2 V^{-1} s^{-1}) compared to the blend films without any post-processing (1.81×10^{-4} and 2.16×10^{-4} cm^2 V^{-1} s^{-1}). The relatively higher charge mobilities of holes and electrons are beneficial to achieve higher J_{sc} and FF values for the PSCs.

AFM and TEM morphologies

To gain further insight into the surface and bulk morphologies of the active layer, atomic force microscopy (AFM) and

Table 1 Photovoltaic performance parameters of the **PIDTV-ffBT**:$PC_{71}BM$-based PSCs under AM 1.5G illumination (100 mW cm^{-2})

D/A [w/w]	V_{oc} [V]	J_{sc} [mA cm^{-2}]	Calculated J_{sc}[a] [mA cm^{-2}]	FF [%]	PCE_{max} [%]
1 : 1	0.73 (0.73 ± 0.01)	13.4 (13.1 ± 0.2)	13.0	59 (57 ± 1)	5.8 (5.5 ± 0.2)
1 : 1.5	0.70 (0.70 ± 0.01)	16.2 (15.7 ± 0.3)	15.6	59 (57 ± 1)	6.7 (6.4 ± 0.1)
1 : 1.5[b]	0.70 (0.70 ± 0.01)	17.1 (16.5 ± 0.3)	16.7	61 (58 ± 2)	7.3 (7.0 ± 0.2)
1 : 2	0.69 (0.69 ± 0.01)	14.6 (14.2 ± 0.1)	14.3	59 (57 ± 1)	6.0 (5.7 ± 0.2)

[a] Calculated by EQE. [b] The PSCs were processed with 1% DIO. The values shown in brackets are the average values with standard deviations of device parameters based on 15 devices.

 This journal is © The Royal Society of Chemistry 2017

Published on 07 February 2017. Downloaded by Osaka University on 20/12/2017 11:40:28.

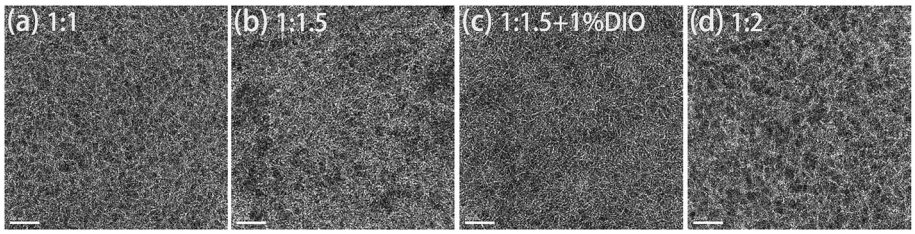

Fig. 4 TEM images of the **PIDTV-ffBT**:$PC_{71}BM$ blend films with different D/A weight ratios without or with 1% DIO.

transmission electron microscopy (TEM) were carried out. Fig. 4 shows the TEM images of the **PIDTV-ffBT**:$PC_{71}BM$ blends with different D/A weight ratios or with 1% DIO. Without any post-processing, all the blend films showed fibrous features, while the blend films showed an increased fibrous structure with the increase of $PC_{71}BM$ content in the active layer. Upon mixing 1% DIO with the blend solution, the **PIDTV-ffBT**:$PC_{71}BM$ (1 : 1.5, w/w) film shows a bicontinuous D/A interpenetrating network with a more suitable fiber size of *ca.* 10 nm and a well-developed and uniform fibrillar morphology compared to the blend film without DIO treatment, which would be beneficial to obtain more efficient exciton dissociation and charge transport for devices, and thus a higher PCE value can be obtained. As shown in Fig. 5, the AFM images of the **PIDTV-ffBT**:$PC_{71}BM$ blend films (1 : 1.5, w/w) without or with 1% DIO confirm the results of the TEM measurements. When 1% DIO was added to the blend solution, the blend film showed a smaller root-mean-square (RMS) roughness value and a more uniform fibrillar structure compared to the blends without DIO. The RMS roughness values are 1.91 and 1.36 nm for the blends processed without and with 1% DIO, respectively.

Conclusions

A novel ladder-type conjugated D–A copolymer **PIDTV-ffBT** based on a 1,1′-vinylene-fused indacenodithiophene (**IDTV**) donor unit was synthesized for application as a donor material in PSCs. Compared to other analogue polymers, **PIDTV-ffBT** exhibited excellent planarity and a 22 π-electron fused system leading to enhanced charge carrier mobility and an extended absorption spectrum with a high absorption coefficient. The **PIDTV-ffBT**:$PC_{71}BM$-based PSCs achieved a good PCE of 7.3% with a high J_{sc} of 17.1 mA cm^{-2}, which is the highest J_{sc} reported for PSCs with ladder-type polymers as donor materials. Our

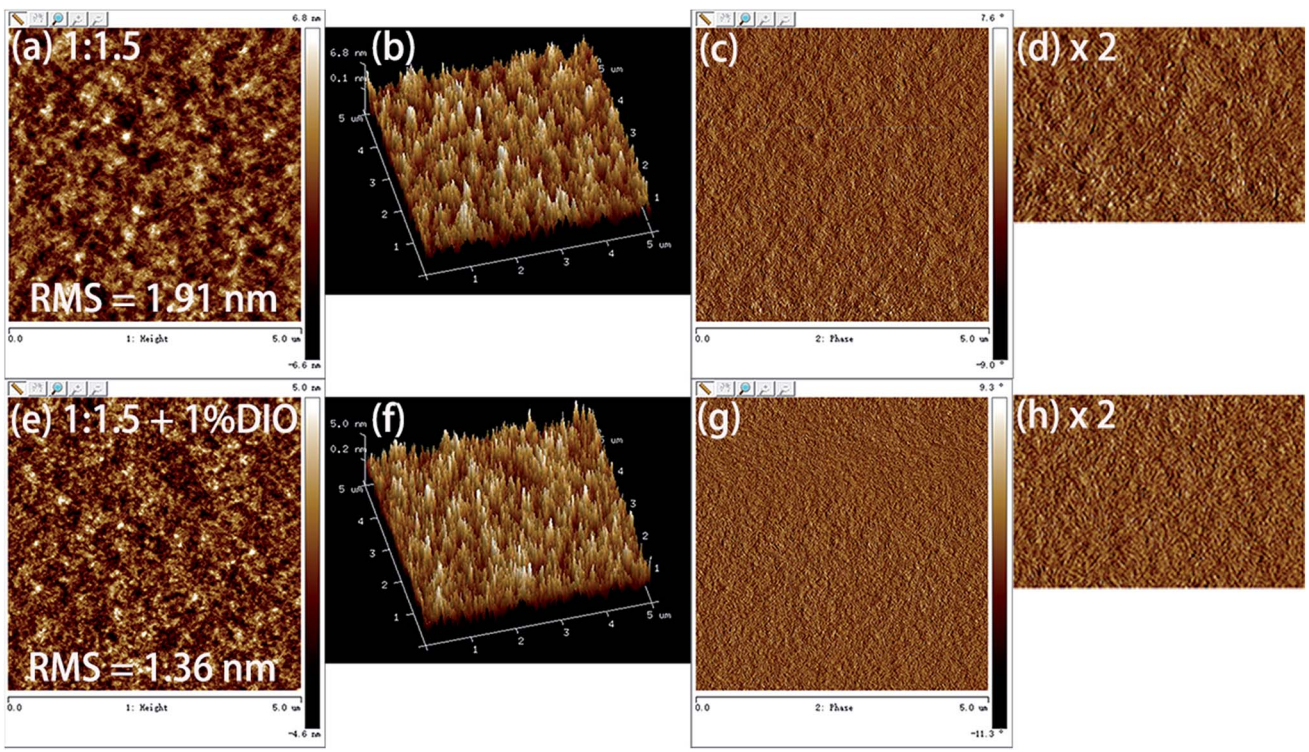

Fig. 5 The AFM images of the **PIDTV-ffBT**:$PC_{71}BM$ blend films without DIO (a–d) and with 1% (v/v) DIO (e–h): (a) and (e) are height images, (b) and (f) are the corresponding two-dimensional height images; (c) and (g) are phase images, (d) and (h) are the corresponding amplification of two times the phase images, respectively.

Published on 07 February 2017. Downloaded by Osaka University on 20/12/2017 11:40:28.

work indicates that the introduction of the 1,1′-vinylene-fused structure into the **IDTV** unit for ladder-type polymers is an effective strategy to enhance the light absorption coefficient and improve charge carrier mobility for efficient PSCs.

Experimental section

Materials

All chemicals and solvents were of reagent grade and purchased from Aldrich, Alfa Aesar and TCI. Compound **ffBT-Br** was purchased from Suna Tech Inc. 4,9-Dihydro-*s*-indacenodithiophene-4,9-dione (**1**) was synthesized according to the procedure reported in the literature.[33] Compounds **IDTV**[31] and **IDTV-Sn** and polymer **PIDTV-ffBT** were synthesized according to Scheme 1.

Synthesis of the compound IDTV

4,9-Dihydro-*s*-indacenodithiophene-4,9-dione (**1**, 5.9 g, 20 mmol) and 100 mL dry *o*-DCB were added into a 250 mL flask under argon and stirred for 0.5 h at room temperature (RT). Then, the freshly prepared Grignard reagent (2-hexyldecyl) magnesium bromide (120 mmol) in 80 mL tetrahydrofuran (THF) was slowly added to the *o*-DCB solution mixture containing compound **1**. The obtained mixture was stirred overnight, and then the mixture was carefully poured into 100 mL ice water, and extracted with ethyl acetate. The organic phase was washed with water and dried over anhydrous $MgSO_4$, and then the solvent was removed by rotary evaporation under low pressure. Then, the residue, 90 mL ethanol, 30 mL hydrochloric acid solution and 60 mL THF were added into a 250 mL flask under argon and stirred for 8 h at 80 °C. After cooling to RT, the mixture was poured into 150 mL distilled water and extracted with petroleum ether (PE). The organic phase was dried over anhydrous $MgSO_4$ and the solvent was removed by rotary evaporation. The residue was purified by silica gel column chromatography using PE as the eluent to obtain compound **IDTV** as a yellow solid (2.8 g, yield 20%). ^{1}H NMR (400 MHz, $CDCl_3$, TMS), δ (ppm): 7.64 (s, 2H), 7.33 (d, $J = 4.8$ Hz, 2H), 7.23 (d, $J = 4.9$ Hz, 2H), 6.35 (d, $J = 10.3$ Hz, 2H), 3.04–3.02 (m, 2H), 1.64–1.62 (m, 8H), 1.47–1.45 (m, 8H), 1.31–1.26 (m, 32H), 0.88–0.81 (m, 12H). ^{13}C NMR (100 MHz, $CDCl_3$, TMS), (ppm): 145.00, 142.31, 140.81, 134.57, 132.97, 132.63, 125.82, 122.49, 110.43, 40.36, 35.95, 31.81, 31.74, 29.96, 29.90, 29.57, 29.53, 29.47, 29.28, 27.58, 27.55, 22.62, 14.06, 14.03. MALDI-TOF MS (*m*/*z*) for $C_{48}H_{70}S_2$, calcd: 710.49, found: 710.41.

Synthesis of the compound IDTV-Sn

LDA (3.5 mL, 2 M in hexane) was slowly added dropwise to a solution of compound **IDTV** (2.0 g, 2.8 mmol) in 30 mL dry THF at −78 °C under argon protection. The mixture was kept at −78 °C for 1.5 h; then, trimethyltin chloride (8.4 mL, 1 M in hexane) was added and the mixture was stirred overnight at RT. The mixture was poured into 100 mL water and extracted with diethyl ether, and the combined organic phase was washed with water and dried over anhydrous $MgSO_4$. The solvent was removed and the crude product was recrystallized with ethanol two times to obtain **IDTV-Sn** as light-yellow crystals (2.3 g, yield 79%). ^{1}H NMR (400 MHz, $CDCl_3$, TMS), δ (ppm): 7.61 (s, 2H), 7.34 (s, 2H), 6.32 (d, $J = 10.2$ Hz, 2H), 3.06–3.04 (m, 2H), 1.64–1.61 (m, 8H), 1.48–1.46 (m, 8H), 1.28–1.22 (m, 32H), 0.85–0.83 (m, 12H), 0.42 (s, 18H). ^{13}C NMR (100 MHz, $CDCl_3$, TMS), (ppm): 151.10, 144.61, 141.20, 139.19, 132.84, 132.33, 130.56, 129.46, 111.22, 40.72, 39.88, 36.75, 35.93, 35.10, 31.84, 29.96, 29.57, 29.35, 28.42, 27.59, 26.76, 22.67, 14.50, 13.68, 8.55. MALDI-TOF MS (*m*/*z*) for $C_{54}H_{86}S_2Sn_2$, calcd: 1036.42, found: 1036.33.

Synthesis of the polymer PIDTV-ffBT

In a dry 50 mL flask, tris(dibenzylideneacetone)dipalladium(0) (3.5 mg) and tri(*o*-tolyl)phosphine (5.1 mg) were added to a solution of **IDTV-Sn** (200 mg, 0.2 mmol) and **ffBT-Br** (64 mg, 0.2 mmol) in 12 mL degassed toluene under argon and stirred vigorously at 110 °C for 1.5 h. Then the mixture was poured into methanol (100 mL) leading to precipitation. The collected polymer was dried and dissolved in *o*-DCB, and then the solution was filtered through a silica gel column. The collected *o*-DCB solution was concentrated and precipitated with methanol to get a dark solid (124 mg, 71%). GPC: $M_n = 28.0$ kDa; $M_w = 90.7$ kDa; PDI = 3.24. Anal. calcd for $C_{54}H_{70}F_2N_2S_3$ (%): C, 73.59; H, 8.01. Found (%): C, 72.81; H, 8.49.

Acknowledgements

This work was supported by the National Natural Science Foundation of China (NSFC) (No. 51422306, 51503135, 51573120 and 91333204), the Priority Academic Program Development of Jiangsu Higher Education Institutions, the Jiangsu Provincial Natural Science Foundation (Grant No. BK20150332), the Natural Science Foundation of the Jiangsu Higher Education Institutions of China (Grant No. 15KJB430027) and the Ministry of Science and Technology of China (973 project, No. 2014CB643501).

Notes and references

1 J.-S. Wu, S.-W. Cheng, Y.-J. Cheng and C.-S. Hsu, *Chem. Soc. Rev.*, 2015, **44**, 1113.
2 (*a*) Y. F. Li, *Acc. Chem. Res.*, 2012, **45**, 723; (*b*) Z.-G. Zhang and Y. F. Li, *Sci. China: Chem.*, 2015, **58**, 192.
3 (*a*) Y. Huang, E. J. Kramer, A. J. Heeger and G. C. Bazan, *Chem. Rev.*, 2014, **114**, 7006; (*b*) L. Y. Lu, T. Y. Zheng, Q. H. Wu, A. M. Schneider, D. L. Zhao and L. P. Yu, *Chem. Rev.*, 2015, **115**, 12666.
4 (*a*) G. P. Luo, X. G. Ren, S. Zhang, H. B. Wu, W. C. H. Choy, Z. C. He and Y. Cao, *Small*, 2016, **12**, 1547; (*b*) S. Q. Zhang, L. Ye and J. H. Hou, *Adv. Energy Mater.*, 2016, **6**, 1502529.
5 J. B. Zhao, Y. K. Li, G. F. Yang, K. Jiang, H. R. Lin, H. Ade, W. Ma and H. Yan, *Nat. Energy*, 2016, **1**, 15027.
6 K. Kawashima, T. Fukuhara, Y. Suda, Y. Suzuki, T. Koganezawa, H. Yoshida, H. Ohkita, I. Osaka and K. Takimiya, *J. Am. Chem. Soc.*, 2016, **138**, 10265.
7 S. Q. Zhang, L. Ye, W. C. Zhao, B. Yang, Q. Wang and J. H. Hou, *Sci. China: Chem.*, 2015, **58**, 248.

 This journal is © The Royal Society of Chemistry 2017

Published on 07 February 2017. Downloaded by Osaka University on 20/12/2017 11:40:28.

8 J. Q. Zhang, Y. J. Zhang, J. Fang, K. Lu, Z. Y. Wang, W. Ma and Z. X. Wei, *J. Am. Chem. Soc.*, 2015, **137**, 8176.
9 (*a*) A. R. B. M. Yusoff, D. Kim, H. P. Kim, F. K. Shneider, W. J. D. Silva and J. Jang, *Energy Environ. Sci.*, 2015, **8**, 303; (*b*) C.-C. Chen, W.-H. Chang, K. Yoshimura, K. Ohya, J. B. You, J. Gao, Z. R. Hong and Y. Yang, *Adv. Mater.*, 2014, **26**, 5670.
10 Z. Zheng, S. Q. Zhang, J. Q. Zhang, Y. P. Qin, W. N. Li, R. N. Yu, Z. X. Wei and J. H. Hou, *Adv. Mater.*, 2016, **28**, 5133.
11 H. Q. Zhou, Y. Zhang, C.-K. Mai, S. D. Collins, G. C. Bazan, T.-Q. Nguyen and A. J. Heeger, *Adv. Mater.*, 2015, **27**, 1767.
12 (*a*) M. J. Zhang, X. Guo, S. Q. Zhang and J. H. Hou, *Adv. Mater.*, 2014, **26**, 1118; (*b*) M. J. Zhang, X. Guo, W. Ma, H. Ade and J. H. Hou, *Adv. Mater.*, 2015, **27**, 4655.
13 (*a*) H. Choi, S.-J. Ko, T. Kim, P.-O. Morin, B. Walker, B. H. Lee, M. Leclerc, J. Y. Kim and A. J. Heeger, *Adv. Mater.*, 2015, **27**, 3318; (*b*) W. W. Li, K. H. Hendriks, A. Furlan, W. S. C. Roelofs, S. C. J. Meskers, M. M. Wienk and R. A. J. Janssen, *Adv. Mater.*, 2014, **26**, 1565.
14 (*a*) Q. P. Fan, W. Y. Su, X. Guo, B. Guo, W. B. Li, Y. D. Zhang, K. Wang, M. J. Zhang and Y. F. Li, *Adv. Energy Mater.*, 2016, **6**, 1600430; (*b*) W. Y. Su, Q. P. Fan, X. Guo, B. Guo, W. B. Li, Y. D. Zhang, M. J. Zhang and Y. F. Li, *J. Mater. Chem. A*, 2016, **4**, 14752; (*c*) Q. P. Fan, Y. Liu, P. G. Yang, W. Y. Su, M. J. Xiao, R. Q. Yang and W. G. Zhu, *Org. Electron.*, 2015, **23**, 124.
15 (*a*) W. T. Li, S. Albrecht, L. Q. Yang, S. Roland, J. R. Tumbleston, T. McAfee, L. Yan, M. A. Kelly, H. Ade, D. Neher and W. You, *J. Am. Chem. Soc.*, 2014, **136**, 15566; (*b*) X. Guo, C. H. Cui, M. J. Zhang, L. J. Huo, Y. Huang, J. H. Hou and Y. F. Li, *Energy Environ. Sci.*, 2012, **5**, 7943.
16 Z. J. Li, K. Feng, J. Mei, Y. Li and Q. Peng, *J. Mater. Chem. A*, 2016, **4**, 7372.
17 (*a*) Q. P. Fan, Y. Liu, M. J. Xiao, W. Y. Su, R. Q. Yang and W. G. Zhu, *Org. Electron.*, 2014, **15**, 3375; (*b*) Q. P. Fan, Y. Liu, M. J. Xiao, W. Y. Su, R. Q. Yang and W. G. Zhu, *J. Mater. Chem. C*, 2015, **3**, 6240; (*c*) Q. P. Fan, X. P. Xu, Y. Liu, W. Y. Su, Q. Peng and W. G. Zhu, *Polym. Chem.*, 2016, **7**, 1747; (*d*) W. Y. Su, Q. P. Fan, M. J. Xiao, H. Tan, Y. Liu, R. Q. Yang and W. G. Zhu, *Macromol. Chem. Phys.*, 2014, **215**, 2075.
18 (*a*) W. Yue, R. S. Ashraf, C. B. Nielsen, S. A. Yousaf, M. Kirkus, H.-Y. Chen, A. Amassian, J. R. Durrant and I. McCulloch, *Adv. Mater.*, 2015, **27**, 4702; (*b*) Z. Y. Zhang, F. Lin, H.-C. Chen, C. Lu, S.-H. Liu, S.-H. Tung, W.-C. Chen, K.-T. Wong and P.-T. Chou, *Energy Environ. Sci.*, 2015, **8**, 552; (*c*) H. A. Saadeh, L. Y. Lu, F. He, J. E. Bullock, W. Wang, B. Carsten and L. P. Yu, *ACS Macro Lett.*, 2012, **1**, 361.
19 (*a*) W. Y. Su, M. J. Xiao, Q. P. Fan, Y. Liu and W. G. Zhu, *Org. Electron.*, 2015, **17**, 129; (*b*) Q. P. Fan, M. J. Xiao, Y. Liu, W. Y. Su, R. Q. Yang and W. G. Zhu, *Polym. Chem.*, 2015, **6**, 4290; (*c*) Q. P. Fan, H. X. Jiang, Y. Liu, W. Y. Su, R. Q. Yang and W. G. Zhu, *J. Mater. Chem. C*, 2016, **4**, 2606; (*d*) Q. P. Fan, Y. Liu, H. X. Jiang, W. Y. Su, R. Q. Yang and W. G. Zhu, *Org. Electron.*, 2016, **33**, 128.
20 C. H. Cui, Z. C. He, Y. Wu, X. Cheng, H. B. Wu, Y. F. Li, Y. Cao and W.-Y. Wong, *Energy Environ. Sci.*, 2016, **9**, 885.
21 (*a*) D. F. Dang, W. C. Chen, Q. Tao, A. Lundin, R. Q. Yang, W. G. Zhu, C. Müller and E. G. Wang, *Adv. Energy Mater.*, 2014, **4**, 1400680; (*b*) X. Guo, M. J. Zhang, J. H. Tan, S. Q. Zhang, L. J. Huo, W. P. Hu, Y. F. Li and J. H. Hou, *Adv. Mater.*, 2012, **24**, 6536.
22 (*a*) Y.-X. Xu, C.-C. Chueh, H.-L. Yip, F.-Z. Ding, Y.-X. Li, C.-Z. Li, X. S. Li, W.-C. Chen and A. K.-Y. Jen, *Adv. Mater.*, 2012, **24**, 6356; (*b*) J. J. Intemann, K. Yao, Y.-X. Li, H.-L. Yip, P.-W. Liang, C.-C. Chueh, F.-Z. Ding, X. Yang, X. S. Li, Y. W. Chen and A. K.-Y. Jen, *Adv. Funct. Mater.*, 2014, **24**, 1465.
23 (*a*) I. McCulloch, R. S. Ashraf, L. Biniek, H. Bronstein, C. Combe, J. E. Donaghey, D. I. James, C. B. Nielsen, B. C. Schroeder and W. M. Zhang, *Acc. Chem. Res.*, 2012, **45**, 714; (*b*) R. S. Ashraf, B. C. Schroeder, H. A. Bronstein, Z. G. Huang, S. Thomas, R. J. Kline, C. J. Brabec, P. Rannou, T. D. Anthopoulos, J. R. Durrant and I. McCulloch, *Adv. Mater.*, 2013, **25**, 2029.
24 (*a*) H. Bronstein, D. S. Leem, R. Hamilton, P. Woebkenberg, S. King, W. M. Zhang, R. S. Ashraf, M. Heeney, T. D. Anthopoulos, J. D. Mello and I. McCulloch, *Macromolecules*, 2011, **44**, 6649; (*b*) X. F. Xu, Z. J. Li, O. Backe, K. Bini, D. I. James, E. Olsson, M. R. Andersson and E. G. Wang, *J. Mater. Chem. A*, 2014, **2**, 18988; (*c*) S. S. Chen, K. C. Lee, Z.-G. Zhang, D. S. Kim, Y. F. Li and C. Yang, *Macromolecules*, 2016, **49**, 527.
25 (*a*) Y. X. Li, K. Yao, H.-L. Yip, F.-Z. Ding, Y.-X. Xu, X. S. Li, Y. Chen and A. K.-Y. Jen, *Adv. Funct. Mater.*, 2014, **24**, 3631; (*b*) Y.-J. Cheng, C.-H. Chen, Y.-S. Lin, C.-Y. Chang and C.-S. Hsu, *Chem. Mater.*, 2011, **23**, 5068.
26 (*a*) Y.-C. Chen, C.-Y. Yu, Y.-L. Fan, L.-I. Hung, C.-P. Chen and C. Ting, *Chem. Commun.*, 2010, **46**, 6503; (*b*) Y. Zhang, S.-C. Chien, K.-S. Chen, H.-L. Yip, Y. Sun, J. A. Davies, F.-C. Chen and A. K.-Y. Jen, *Chem. Commun.*, 2011, **47**, 11026.
27 (*a*) M. J. Zhang, X. Guo, C. Wang, H. Q. Wang and Y. F. Li, *Chem. Mater.*, 2011, **23**, 4264; (*b*) M. Wang, H. B. Wang, T. Yokoyama, X. F. Liu, Y. Huang, Y. Zhang, T.-Q. Nguyen, S. Aramaki and G. C. Bazan, *J. Am. Chem. Soc.*, 2014, **136**, 12576.
28 (*a*) Y. Zhang, J. Y. Zou, H.-L. Yip, K.-S. Chen, D. F. Zeigler, Y. Sun and A. K.-Y. Jen, *Chem. Mater.*, 2011, **23**, 2289; (*b*) R. F. He, L. Yu, P. Cai, F. Peng, J. Xu, L. Ying, J. W. Chen, W. Yang and Y. Cao, *Macromolecules*, 2014, **47**, 2921.
29 (*a*) C. Du, C. H. Li, W. W. Li, X. Chen, Z. S. Bo, C. Veit, Z. F. Ma, U. Wuerfel, H. F. Zhu, W. P. Hu and F. L. Zhang, *Macromolecules*, 2011, **44**, 7617; (*b*) M. Heeney, C. Bailey, M. Giles, M. Shkunov, D. Sparrowe, S. Tierney, W. M. Zhang and I. McCulloch, *Macromolecules*, 2004, **37**, 5250.
30 W. W. Li, K. H. Hendriks, M. M. Wienk and R. J. Janssen, *Acc. Chem. Res.*, 2016, **49**, 78.
31 (*a*) Y. J. Xia and D. W. Fan, CN Pat., 102643284 A, 2012; (*b*) C. S. Wang, N. Blouin, M. Dlavari, S. Tierney and L. Nanson, WO Pat., 2013000532 A1, 2013.

32 (*a*) B. A. Collins, Z. Li, J. R. Tumbleston, E. Gann, C. R. McNeill and H. Ade, *Adv. Energy Mater.*, 2013, **3**, 65; (*b*) X. H. Lu, H. Hlaing, D. S. Germack, W. H. Jo, D. Andrienko, K. Kremer and B. M. Ocko, *Nat. Commun.*, 2012, **3**, 795.
33 W. M. Zhang, J. Smith, S. E. Watkins, R. Gysel, M. McGehee, A. Salleo, J. Kirkpatrick, S. Ashraf, M. Heeney and I. McCulloch, *J. Am. Chem. Soc.*, 2010, **132**, 11437.
34 L. J. Huo, T. Liu, X. B. Sun, Y. H. Cai, A. J. Heeger and Y. M. Sun, *Adv. Mater.*, 2015, **27**, 2938.
35 P. W. M. Blom, V. D. Mihailetchi, L. J. A. Koster and D. E. Markov, *Adv. Mater.*, 2007, **19**, 1551.
36 S. R. Cowan, A. Roy and A. J. Heeger, *Phys. Rev. B: Condens. Matter Mater. Phys.*, 2010, **82**, 245207.

Published on 07 February 2017. Downloaded by Osaka University on 20/12/2017 11:40:28.

This journal is © The Royal Society of Chemistry 2017